JOURNAL OF SPACECRAFT AND ROCKETS
Vol. 46, No. 5, September–October 2009

Stochastic Analysis of Constellation Performance and Mass Margins

Brian K. Muirhead,* Robert Shishko,† and George Fox‡
Jet Propulsion Laboratory, California Institute of Technology, Pasadena, California 91109

DOI: 10.2514/1.40243

A new method for analyzing margins in the Constellation program is described and applied to the performance and mass margins for the integrated transportation system returning humans to the lunar surface. The approach treats the Ares-V Earth-departure-stage gross payload-delivery capability and the translunar injection masses of Orion and Altair as random variables. For various vehicle requirements, vehicle control masses, and design reference missions, a Monte Carlo simulation estimate is used to estimate the critical probability that the delivery capability exceeds that injected mass. This critical probability can be used to establish program performance and mass margins and, in conjunction with other measures, to manage vehicle selection and trades at the program level.

Nomenclature

$F(\ldots)$, $G(\ldots)$	=	cumulative distribution functions
$f(\ldots)$, $g(\ldots)$, $\zeta(\ldots)$	=	probability density functions
I_{sp}	=	specific impulse, s
$\lvert J \rvert$	=	absolute value of the transformation Jacobian
M^t_{TLI}	=	translunar injection stack mass, kg, estimated at time t
P^t_{EDS}	=	Ares-V Earth-departure-stage gross payload-delivery capability, kg, estimated at time t
β	=	mass growth coefficient
Δv	=	maneuver change in velocity
ε	=	normally distributed error term

I. Introduction

ESTABLISHING and managing margin requirements provides a way for programs to better their chances of meeting key performance and physical parameters in the face of uncertainties. These margin requirements provide resiliency against less-than-favorable outcomes during system development and mitigate risks inherent in complex space missions. During development, technical managers can compare the actual margin against the margin requirement and take corrective action as necessary. The actual margin at time t is generally defined as the difference between the measured (or demonstrated) value for a key performance or physical parameter and its controlled (or allocated) value at that time. Typically, as remaining uncertainties diminish, so do margin requirements, reaching or approaching zero at the completion of the development cycle.

The Constellation program is an immense undertaking involving the development of a number of new systems designed to enable crew transfers to the International Space Station, a human lunar return, establishment of an outpost on the moon, and an eventual human voyage to Mars. The systems being developed (Orion, Altair, Ares-I, and Ares-V among them) must work together to provide transportation for both crew and cargo in a complex supply chain. The physics of space travel makes it necessary to carefully assess the launch vehicle performance and spacecraft masses throughout development to ensure that this system-of-systems is capable of meeting the top-level program requirements. To this end, a new type of integrated analysis was performed, treating both performance and spacecraft masses stochastically. Such an analysis was suggested by Shishko and Chamberlain [1].

The principal question addressed by the analysis was simply, "Does Constellation have a sufficient mass margin across program elements to ensure that Ares-V performance will exceed the stack mass at translunar injection (TLI) with high probability?" Though the analysis approach can be applied generally, the analysis described in this paper was performed for the Constellation lunar sortie Design Reference Mission (DRM). In that DRM, the Ares-V is the launch vehicle for the Altair lunar lander and includes an upper stage, known as the Earth departure stage (EDS). The EDS provides the Δv for both orbit circularization and then TLI, once the Orion crew vehicle, launched separately on the Ares-I, docks with Altair. In this paper, the performance of the Ares-V/EDS is its gross payload-delivery capability measured kilograms. The payload is defined as the total injected mass at the end of TLI less the burnout mass of the EDS. The TLI stack consists of the Altair, Orion, and the Altair-to-EDS spacecraft adapter.

Figure 1 is a depiction of the Constellation lunar sortie DRM. Lunar sorties are representative of Apollo-style missions that enable crew members to explore a single site anywhere on the moon with the length of stay limited by the amount of consumables brought by the lander and Δv margins. Aside from the larger crew size and the length of stay on the lunar surface planned by the Constellation program, there are several key differences between the Constellation and Apollo lunar sortie DRMs. One is the use in Constellation of separate launches for Orion and Altair and their subsequent docking in an Earth rendezvous orbit. The other key difference is the use of Altair's main engine to perform lunar orbit insertion (LOI), in contrast to Apollo's use of its service module (SM).

II. Basic Concepts

Setting the program manager reserve (PgMR) and project manager reserve(s) (PMR) in the Constellation program is part of the margin management process. Figure 2 provides the canonical view of mass margin concepts used in the Constellation program. Analysis of requirements associated with performing a variety of DRMs helps to establish control masses for each element of the TLI stack. Typically, the project manager for each element establishes a (time-phased)

Received 4 August 2008; revision received 20 March 2009; accepted for publication 18 March 2009.

*Constellation Program Systems Engineer. Member AIAA.
†Principal Systems Engineer/Economist, Mission/System Concepts Section. Member AIAA.
‡Senior Software Engineer, Mission/System Concepts Section.

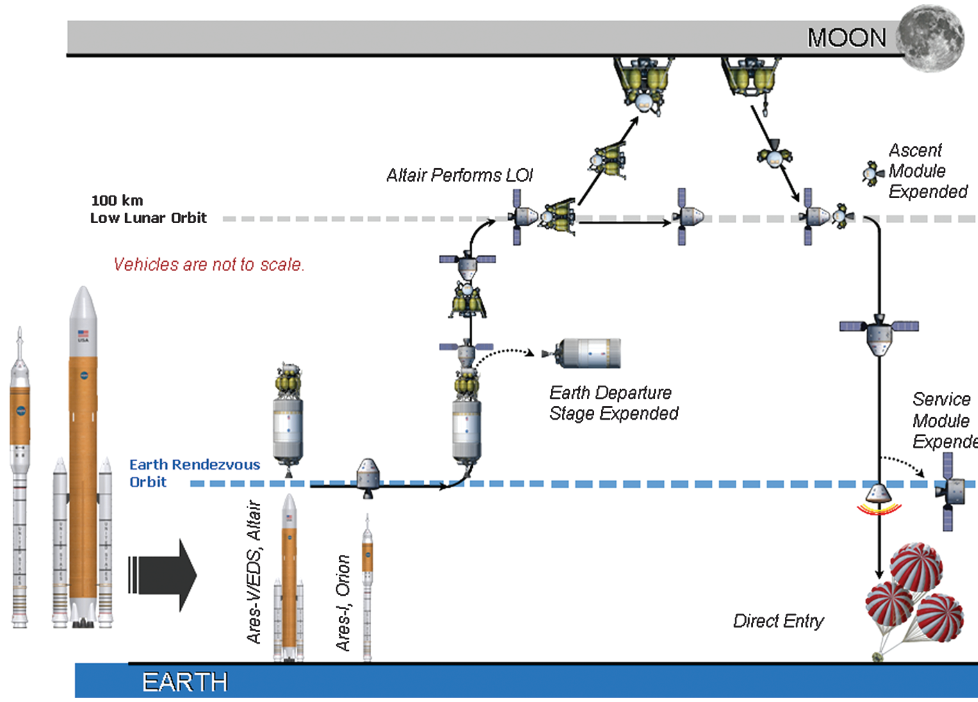

Fig. 1 Constellation lunar sortie DRM.

required mass reserve to be held at the project level in case of in-scope requirement changes and potential threats and opportunities. The design organizations then begin the design process, targeting the control mass less the current project-level mass reserve. Against a given baseline design, design organizations typically apply (time-phased) mass growth allowances (MGAs) based on rules-of-thumb and organizational experience with similar previous projects [2]. MGA is meant to cover typical mass growth associated with the baseline design as it matures from concept to hardware. In practice, it may be allocated to lower-level systems and subsystems, held at a higher level, or a combination of both approaches. The resulting predicted mass (basic mass plus MGA) plus the current PMR requirement is then compared with the control mass, providing the measure of residual project mass margin. Whenever this residual is negative (or judged to be insufficient due to threats), then corrective action is needed.

The approach described in this paper took the view that the TLI stack mass could better be represented as a probability distribution, rather than as a nonstochastic predicted mass. Similarly, instead of representing the gross payload-delivery capability of the Ares-V/EDS as a single calculated value, the new approach represented it as a probability distribution. Notional distributions for these two are shown in Fig. 2 on the right. (How the probability distributions were actually developed for Constellation will be described shortly.) Of critical interest to the Constellation program was the probability distribution for the difference between the Ares-V/EDS performance and the TLI stack mass (i.e., for the total residual mass and performance margin).

Let P^t_{EDS} be the (actual final) gross capability of the Ares-V/EDS, $f(\ldots)$ its probability density function (PDF), M^t_{TLI} the (actual final) TLI stack mass, and $g(\ldots)$ its corresponding PDF. Both P^t_{EDS} and M^t_{TLI} depend implicitly on a multitude of design decisions based on

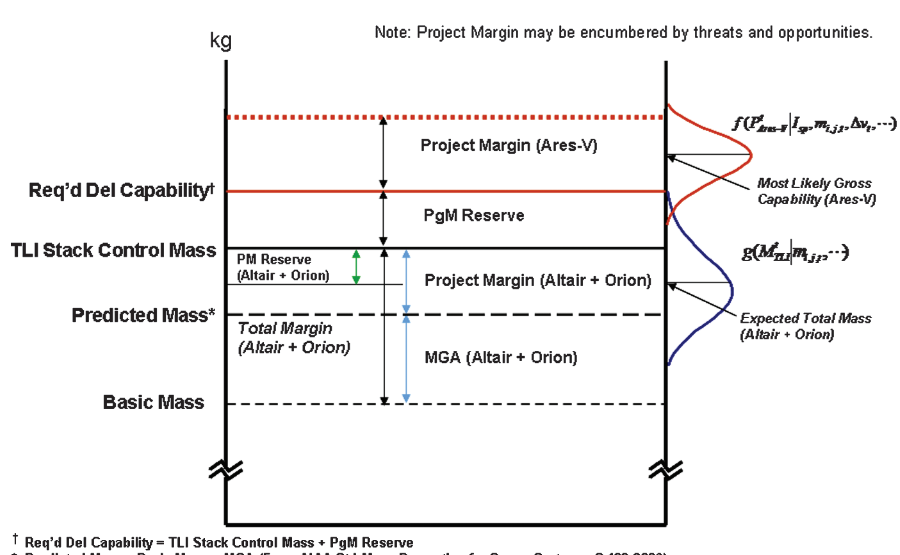

Fig. 2 Controlled values, hypothetical stochastic mass and performance estimates, and margin relationships.

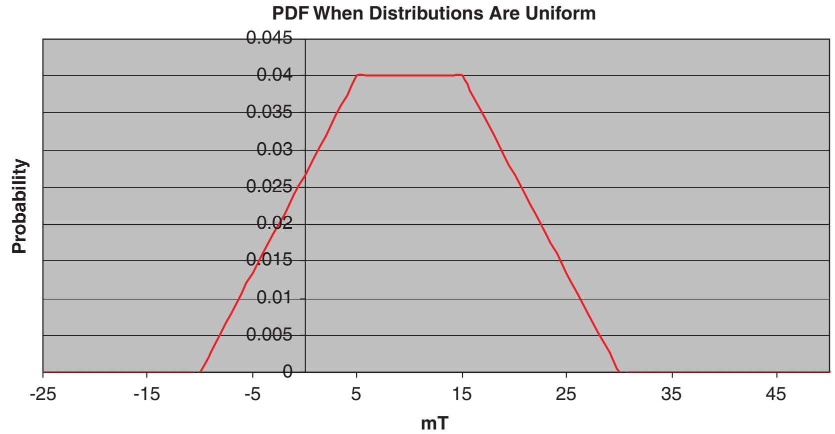

a)

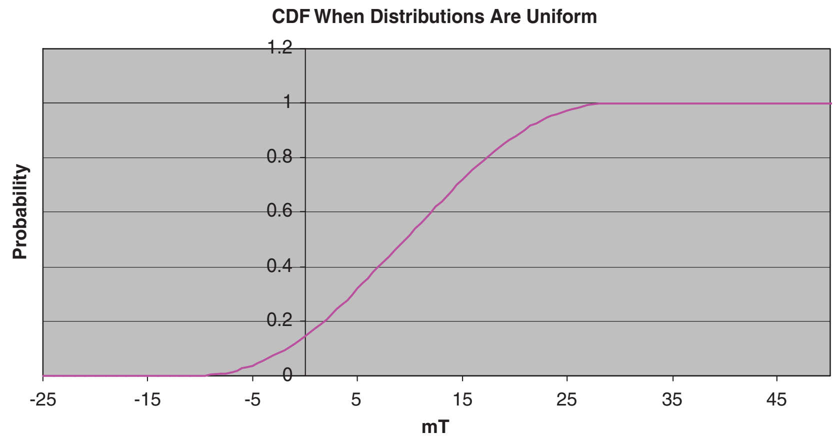

b)

Fig. 3 Gross capability less TLI stack mass when both are uniformly distributed: a) illustrative PDF and b) illustrative CDF.

system requirements. For example, the gross capability of the Ares-V/EDS is a function of the configuration, design, and the performance characteristics of its various rocket engines, and the TLI stack mass is a rollup of the masses of its component systems, modules, and subsystems. These system, module, and subsystem masses are in turn driven by requirements on crew size, mission duration, habitability, reliability, and mission Δv and by the resulting design choices such as engine types and associated I_{sp}. Varying degrees of performance and mass uncertainty are present in each proposed design at the outset of the development process, but the PDFs for P^t_{EDS} and M^t_{TLI} are effectively decoupled once requirements and the resulting basic designs are fixed. For this reason, the assumption was made in the analysis that P^t_{EDS} and M^t_{TLI} are stochastically independent.[§]

To calculate the marginal of $P^t_{\mathrm{EDS}} - M^t_{\mathrm{TLI}}$, define $y_1 = P^t_{\mathrm{EDS}} - M^t_{\mathrm{TLI}}$ and $y_2 = M^t_{\mathrm{TLI}}$. The desired PDF is then given by

$$\xi(y_1) = \int_0^\infty f(y_1 + y_2) g(y_2) |J| \mathrm{d}y_2 \tag{1}$$

where the absolute value of the Jacobian $|J|$ for this transformation is just 1.

This marginal PDF was calculated for the Constellation lunar transportation system-of-systems by Monte Carlo simulation, to be described later, but for simple cases, it can be done analytically. Suppose, for the sake of illustration, that the gross capability and TLI stack mass PDFs are both uniform: in particular, $f(\ldots) \sim U(55, 80)$ and $g(\ldots) \sim U(50, 65)$. Because they overlap in the range between 55 and 65 t, there is some probability that the difference y_1 will be negative. The result of applying Eq. (1) to these hypothetical distributions is shown in Fig. 3a, and the corresponding cumulative distribution function (CDF) is shown in Fig. 3b.

As can be seen from Fig. 3b, the probability that the gross capability will be insufficient (i.e., less than the TLI stack mass) is about 13% in this example. If the established PgMR in this example is, say, 5 t, then the probability that at least some of that reserve will be consumed is 30%.

In practice, providing credible probability distributions for the actual final values of Ares-V/EDS gross capability and the TLI stack mass relied on a combination of historical data, expert probability assessment, modeling, and Monte Carlo simulation. These efforts are discussed subsequently.

§Random variables X and Y are said to be stochastically independent if and only if $f(x, y) = f_X(x) f_Y(y)$.

III. Generating the TLI Stack Mass PDF

A. Dry Mass Growth

A number of previous researchers have documented mass growth in spacecraft and launch vehicles over the development cycle [3–6]. What was needed to implement the stochastic approach was not only the ability (i.e., a model) to predict the actual TLI mass based on current mass information, but the uncertainty in that estimate. In other words, a mechanism to propagate current basic dry mass estimates stochastically to a TLI mass PDF was needed. Because no flight hardware has been built, current basic dry mass information for the Constellation TLI stack comes from estimates based on a preliminary master equipment list or parametric model for each stack element. To generate a useful model, historical mass data from previous NASA missions were collected. In particular, a time series of basic dry mass estimates was collected using original sources wherever possible, as this provided a means to ensure that consistent definitions were used in what was being reported.

Next, the dates of key milestones in the development program were identified. These key milestones were system requirements review (SRR) (or the equivalent), preliminary design review (PDR), critical design review (CDR), design certification review (DCR), and launch. From a historical perspective, the PDR, CDR, and DCR were institutionalized as formal reviews within NASA's Apollo program only in 1965 [7]. Matching the basic dry mass data to these milestones was important, because projects typically build a formal baseline to support these reviews. For many early projects, identifying the dates for these reviews was not necessarily easy or unambiguous. For example, a formal SRR event for the lunar excursion module (LEM) could not be identified from official NASA chronologies, and so the mass data in Apollo Quarterly Status Report (QSR) No. 4 [8] were taken as the best match to the caliber of information available at the time of an SRR. Quoting from that report [8],

> Grumman Aircraft Engineering Corporation's preliminary Lunar Excursion Module Mass Properties Report was received. The weights shown in the report have since increased as a result of more stringent design requirements, and results emphasize that strict weight control will be required to insure that the control weight is not exceeded. Studies currently being conducted will refine these target values. The Lunar Excursion Module weight increases shown in table IV result primarily from increased velocity requirements and changed specific impulse values of the ascent and descent engines.

The initial basic dry mass time series data collection netted 23 Jet Propulsion Laboratory and NASA Goddard Space Flight Center missions, many of which employed small spacecraft. This data set lacked manned missions, larger spacecraft, and missions managed by other NASA Centers. Consequently, the data set was augmented with Mercury, Gemini, and Apollo [command and service module (CSM) and LEM] data gathered from original sources (e.g., QSRs) [9–58]. The most complete time series on these projects was either inert mass or gross mass, and so it was necessary to apply adjustments (e.g., subtracting crew mass and usable propellant mass) to get as close to basic dry mass as possible. The data set was also augmented with Viking Orbiter/Lander, Voyager, Magellan, Topex/Poseidon, Skylab, Space Shuttle Orbiter, and Hubble Space Telescope data [59–67]. Ultimately, the data set was trimmed to include only those spacecraft for which the dry mass at launch exceeded 500 kg, resulting in $n = 18$ data points.

Three models were proposed relating the (actual) spacecraft dry mass at launch to the basic dry mass estimated at SRR:

$$M_{\text{launch}}^{\text{dry}} = \beta M_{\text{SRR}}^{\text{dry}} + \varepsilon \tag{2}$$

$$M_{\text{launch}}^{\text{dry}} = \beta M_{\text{SRR}}^{\text{dry}} + \varepsilon \sqrt{M_{\text{SRR}}^{\text{dry}}} \tag{3}$$

$$M_{\text{launch}}^{\text{dry}} = \beta M_{\text{SRR}}^{\text{dry}} + \varepsilon M_{\text{SRR}}^{\text{dry}} \tag{4}$$

where $\varepsilon \sim N(0, \sigma^2)$ in all three models. In the first model, represented by Eq. (2), the regression disturbances exhibit a constant variance across observations (homoscedasticity), whereas in the two other models, represented by Eqs. (3) and (4), the regression disturbances exhibit heteroscedasticity (i.e., their variances are not constant across observations). In the second model, the standard deviation grows as the square root of SRR basic dry mass, and in the third model, it grows linearly with SRR basic dry mass. All three models were estimated using the collected data set and tested against the null hypothesis of normality of the regression disturbances using the Anderson–Darling statistic [68]. The procedure is described in [69] (Sec. 1.3.5.14) and the results are reported in Table 1. On this basis, Eq. (4) was selected as the best to use in further analyses. The full time-series data on Gemini and Apollo appear in Tables A1–A6. The full data set used in the analysis appears in Table B1.

Table 1 Anderson–Darling test statistic[a] for proposed models

Model	Anderson–Darling statistic
Equation (2)	2.575
Equation (3)	1.122
Equation (4)	0.281

[a]Critical values for rejecting the null hypothesis of normality are 0.656 (at 10% significance level), 0.787 (5%), and 1.092 (1%).

The estimated mass growth coefficient $\hat{\beta}$ has considerable uncertainty because of the dispersion in the available historical data. Using this average growth to predict the dry mass at launch of a new spacecraft does not fully capture the situation and, if the historical record is a predictor of the future, provides protection from mass growth problems only about half the time in the absence of additional margin. Using the data set, the distribution describing the dry mass at launch based on basic dry mass at the time of SRR was estimated to be

$$\begin{aligned} M_{\text{launch}}^{\text{dry}} &\sim N(\hat{\beta} M_{\text{SRR}}^{\text{dry}}, \sqrt{\hat{s}^2(1+n^{-1})} M_{\text{SRR}}^{\text{dry}}) \\ &\sim N(1.29719 M_{\text{SRR}}^{\text{dry}}, 0.1579 M_{\text{SRR}}^{\text{dry}}) \end{aligned} \tag{5}$$

where $\hat{s}^2$ is an estimate of the true variance from the regression and n is the number of observations in our data set. It is conceivable that combining robotic spacecraft and crewed spacecraft in the same model might not be supportable. The null hypothesis was tested that the regression coefficients would be different for these two samples using a Chow F test. The results strongly indicated that the hypothesis should be rejected. Similarly, one could argue that the ability of project engineers to estimate actual (launch) dry mass at the time of the SRR has gotten better over the course of the past 50 years. The data set was segregated into spacecraft launched before 1985 and those launched after and then tested against the null hypothesis that the regression coefficients would again be different. The results here also indicated that the hypothesis should be rejected.

B. Dry Mass to TLI Mass

The Altair lunar lander consists of three modules: 1) a descent module (DM), which performs the LOI and descent to the lunar surface; 2) an ascent module (AM), which performs ascent and rendezvous with the orbiting Orion; and 3) an airlock module, which provides egress to and ingress from the lunar surface. In the Monte Carlo simulation used to generate the PDF for $P_{\text{EDS}}^{t} - M_{\text{TLI}}^{t}$, the TLI mass of the Altair was sampled from a distribution generated by application of Eq. (5) to the current basic dry mass estimates for each Altair element and from the resulting dry mass at launch, computing its TLI mass using a multistage rocket equation tool called MassTracker [70]. The Altair DM and AM engine I_{sp} were treated as random variables described by triangular distributions. Stochastic mass growth was not applied to the mass of extravehicular activity (EVA) equipment, flight crew equipment (FCE), unpressurized cargo on the DM, unusable propellant, and nonpropellant (usable food, fluids, and gases).[¶] Crew mass was counted in the Orion TLI mass and moved to the Altair AM to calculate decent, ascent, and rendezvous propellant masses in MassTracker. Lunar samples transported in the AM were assumed to be 100 kg in the results reported subsequently.

[¶]This was done to focus the analysis on the transportation vehicles because EVA equipment, FCE, unusable propellant, and nonpropellants are sufficiently well established from previous human spaceflight experience. Though treated deterministically, the EVA equipment mass value contained a mass growth allowance and manager's reserve measured in the tens of kilograms.

MassTracker computes wet mass via the successive reverse application of the rocket equation. It requires external inputs that are determined by the specific lunar mission design. In particular, translation and reaction control Δv were provided by mission designers based on a required set of maneuvers (e.g., LOI, plane changes, descent to the lunar surface, and ascent from the lunar surface). These maneuvers are allocated to specific Altair elements so that MassTracker can compute the postmaneuver element mass and propellant of each type expended. Another externally provided input to MassTracker was the Altair boil-off losses, because this also depends on the specifics of the mission design (e.g., days in low-Earth-orbit loiter). The boil-off model generally consisted of a larger loss rate during an initial cold-soak period following launch and a lesser loss rate thereafter. Both of these external inputs were provided by the Envision model used extensively during and since the Exploration Systems Architecture Study [71].

C. Ares-V/EDS Performance Calculations

The use of historical data to estimate the Ares-V/EDS gross performance PDF was not possible, as there is a serious lack of data on which to build a model equivalent to the dry mass growth model. The process used for the preliminary performance and sizing of Ares-V/EDS concepts is shown in Fig. 4. Based upon the mission requirements for the particular concept under study and within the framework of the ground rules and assumptions established, a preliminary concept is sized using the mass-estimating relationships (MERs) in the INTROS (Integrated Rocket Sizing) program. Using this vehicle, an initial trajectory is flown in POST3D (Program to Optimize Simulated Trajectories) to determine the ascent flight environments (accelerations, dynamic pressure, payload capability, etc.) and then the initial vehicle weights and trajectory outputs are sent to LVA (launch vehicle analysis) for more detailed structural sizing. Loads, forces, material properties, and design techniques are all considered within the LVA analysis, and new structural weights are calculated for the Ares-V/EDS concept. INTROS then incorporates these new structural element weights and estimates a total injected mass based on the total ideal Δv from the previous POST3D output. POST3D then determines a new total injected mass and ideal Δv. INTROS takes these values from POST3D and estimates a new value for propellant reserves and continues to iterate with POST3D until the POST3D total injected mass is within 300 lb (136 kg) of the INTROS estimated value. The performance and sizing analysis for this concept is then considered closed and a vehicle summary is generated. This iterative analysis of a new Ares-V/EDS concept is performed with a team of experts in the loop, rather than as an automated process. The three analysis tools used are subsequently described in more detail.

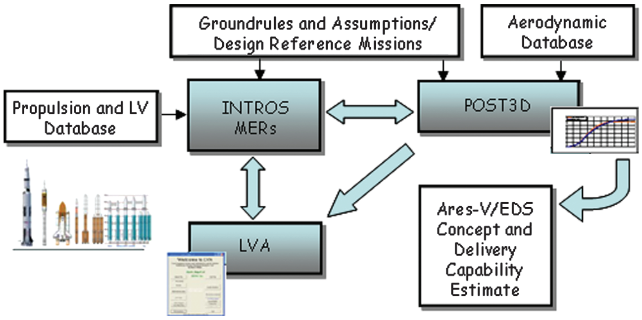

Fig. 4 General description of the iterative process and tools used to determine the performance and size of new Ares-V/EDS concepts (LV denotes launch vehicle).

INTROS is an analytical tool that was developed at the NASA Marshall Space Flight Center (MSFC) to establish launch vehicle designs and sizing. It is written in Visual BASIC for Applications computer language and uses the Excel application for all inputs and outputs. Launch vehicle design and sizing analyses are based on stage geometry and mass properties. These mass properties are established from a large master list of launch vehicle systems, subsystems, propellants, and fluids. Mass calculations are based on MERs that are automatically generated from a large database of MERs that is built into the program. Program mass calculation accuracy for existing and historical launch vehicles has been verified to be well within 5%.

LVA is a standalone application written at MSFC in Visual BASIC that provides extremely fast launch vehicle structural design and analysis. It does not use mass estimating or scaling routines, but rather, it supplies detailed analysis by using time-proven engineering methods based on material properties, load factors, aerodynamic loads, stress, elastic stability, deflection, etc. For the fastest turnaround, the program is designed to work with the absolute minimum of input data. The output data are purposely limited to the least possible quantity to prevent the analyst from having to dig through a large amount of data for the necessary information.

POST3D is a FORTRAN 77-based legacy code developed at the NASA Langley Research Center for detailed trajectory simulations. POST3D provides the capability to target and optimize point mass trajectories for a powered or unpowered vehicle near an arbitrary rotating oblate planet. POST3D has been used successfully to solve a wide variety of atmospheric ascent and reentry problems, as well as

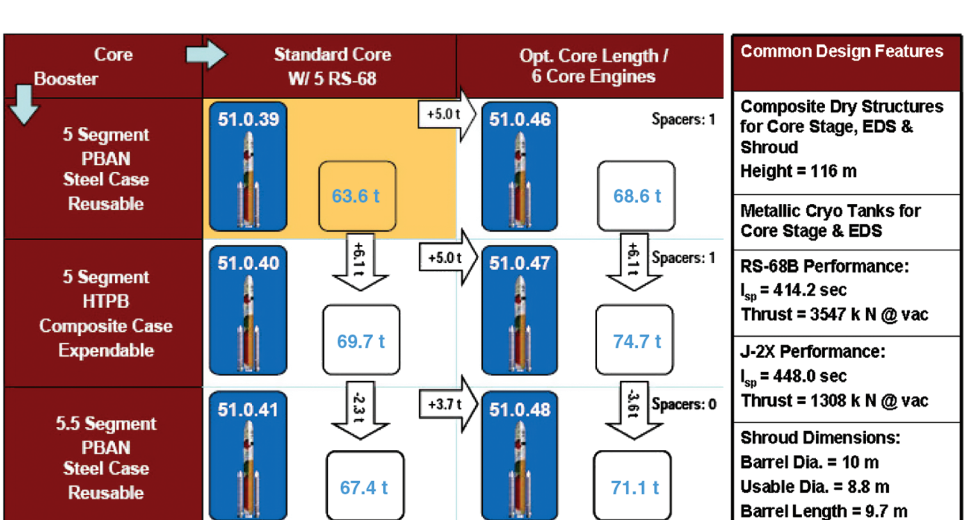

Fig. 5 Tradespace of Ares-V/EDS Series 51 conceptual designs showing early (deterministic) estimates of gross payload delivery at TLI in metric tons next to each picture. The block arrows show the performance changes.

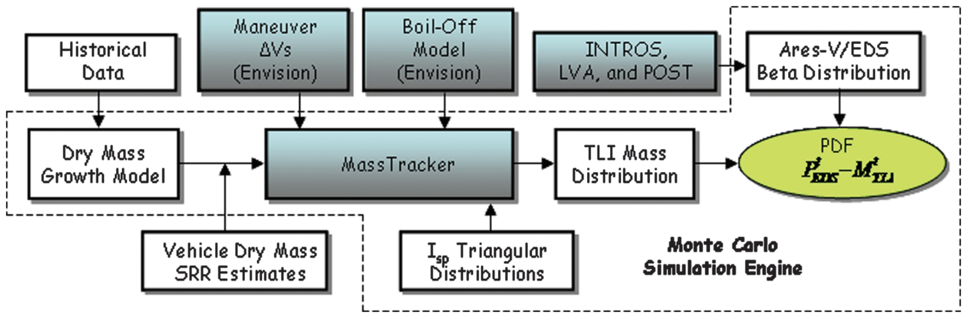

Fig. 6 Analysis flow leading to the PDF for the difference between Ares-V/EDS performance and the TLI stack mass. Shaded boxes represent various software models and simulations used in the analysis.

exoatmospheric orbital transfer problems. The generality of the program is evidenced by its N-phase simulation capability, which features generalized planet and vehicle models. This flexible simulation capability is augmented by an efficient discrete parameter optimization capability that includes equality and inequality constraints [72].

For the Constellation program, a number of new concepts for the Ares-V/EDS have been analyzed, and some of these are described in Fig. 5. Although they share a number of physical dimensions and shuttle-derived technologies, these concepts are distinguished by a number of design characteristics: in particular, the number of RS-68B core-stage engines (5 or 6) and optimized core length, the booster-stage propellant [polybutadiene acrylonitrile (PBAN) or hydroxyl-terminated polybutadiene (HTPB)] and material, and the number of segments (5 or 5.5). The shuttle's solid rocket boosters (SRBs) are composed of four segments. The Ares-I launcher for Orion has five segments, but to lengthen the Ares-V core stage in some concepts, an additional half-segment had to be inserted. The shuttle's SRBs use PBAN propellant in a reusable steel case, but higher thrust and performance can be obtained by using HTPB propellant. An expendable filament-wound composite case rather than a reusable steel case also offers higher performance, but with likely cost penalties for the program.

The stochastic margins analysis reported in this paper focused on three of the six variants of the Series 51 Ares-V/EDS. Common features of the Series 51 include composite dry structures, height and shroud dimensions, and the use of the RS-68B for the core stage and J-2X for the EDS. The RS-68 is a throttlable liquid-hydrogen/liquid-oxygen booster engine for the Delta-IV launch vehicle family. The J-2X, a derivative of the J-2 Apollo era engine, is a restartable engine that also uses liquid hydrogen with liquid oxygen as its propellant.

The 51.0.39 conceptual design represents the lowest gross payload-delivery capability (performance) and lowest development risk among those in Fig. 5. The 51.0.47 conceptual design represents the highest performance and risk, whereas the 51.0.48 conceptual design lies between the other two in the tradespace, both in terms of performance and development risk. The iterative process for performance and sizing, however, does not produce a probability distribution for gross payload-delivery capability. To do so requires that the models and tools used be more closely integrated so that Monte Carlo methods can be applied. Because the difficulty lies in trying to repeatedly apply POST3D in its native FORTRAN code, an obvious approach is to develop a response surface that could credibly act in lieu of POST3D for a given conceptual design. This tactic was used and such detailed response surfaces were prepared by Wallace et al. [73] using a statistical package called JMP®. The resulting response surfaces were imported into Excel, which was then integrated with the other Visual BASIC tools using ModelCenter and executed in a Monte Carlo mode. The techniques employed were similar to those reported in [73].

The process for selecting a stochastic representation of the Ares-V/EDS gross payload-delivery capability at the conceptual stage of project maturity was to elicit probability distribution parameters from recognized experts informed by the results of the just-described Monte Carlo analysis using the sizing and performance tools (INTROS, LVA, and POST3D). A beta distribution, Eq. (6), was chosen as an appropriate portrayal of the gross payload-delivery capability uncertainty for each conceptual design. Several methods are available for translating a limited number of parameters (typically, quantiles) into the full beta distribution [69] (Sec. 1.3.6.6.17) and [74]. The extended Pearson–Tukey approximation described in [75], which relies on elicited values for the 5th, 50th, and 95th percentile values to estimate p and q, was used. As a final step, the resulting full beta distributions were reviewed by the same group of experts.

$$P^t_{\mathrm{EDS}} \sim \mathrm{beta}(p, q, \min, \max) \tag{6}$$

D. Monte Carlo Simulation Results

The end-to-end Monte Carlo analysis flow is shown in Fig. 6. The critical probability of interest to the Constellation program is the probability that the Ares-V/EDS gross payload-delivery capability exceeds the TLI stack mass. A low value for this probability, even early in program formulation, would indicate serious issues in the selection of conceptual designs and mass margins.

A synopsis of the stochastic mass margin analysis flow follows. Given the SRR basic dry mass estimates for Orion and Altair, the Monte Carlo simulation engine draws dry mass values at launch from the distribution represented in the dry mass growth model [Eq. (5)]. These dry mass values at launch are passed to MassTracker, which calculates the resulting TLI stack mass for each trial using lunar mission-specific Δv. The Monte Carlo simulation engine incorporates triangular distributions on the Orion and Altair engines' I_{sp} into the MassTracker analysis. The distributions represent the current best estimates from NASA propulsion experts about what the I_{sp} will be at launch. The most likely values of the triangular distributions were taken to be the advertised minimum, so as not to be overly optimistic.** These I_{sp} distributions were not great contributors to the uncertainty in the TLI stack mass. The dry mass growth model [Eq. (5)] was by far the greatest contributor to that uncertainty. Additional inputs to MassTracker come from the Envision model and these are treated deterministically. As stated earlier, the Ares-V/EDS gross capability PDF is determined by expert judgment conditioned on Monte Carlo analysis using the sizing and performance tools (INTROS, LVA, and POST3D). For each Ares-V/EDS concept, the final PDF is represented as a beta distribution. Finally, the TLI stack

**The I_{sp} distributions in the analysis are very narrow and are expected to become more so as test data are accumulated. For the RL-10-derived DM engine, the triangular distribution parameters were as follows: minimum was 440 s, most likely was 448.56 s, and maximum was 455 s. For the AM engine, the triangular distribution parameters were (318, 320.3, and 326), and for the SM main engine, the parameters were (323, 328, and 331).

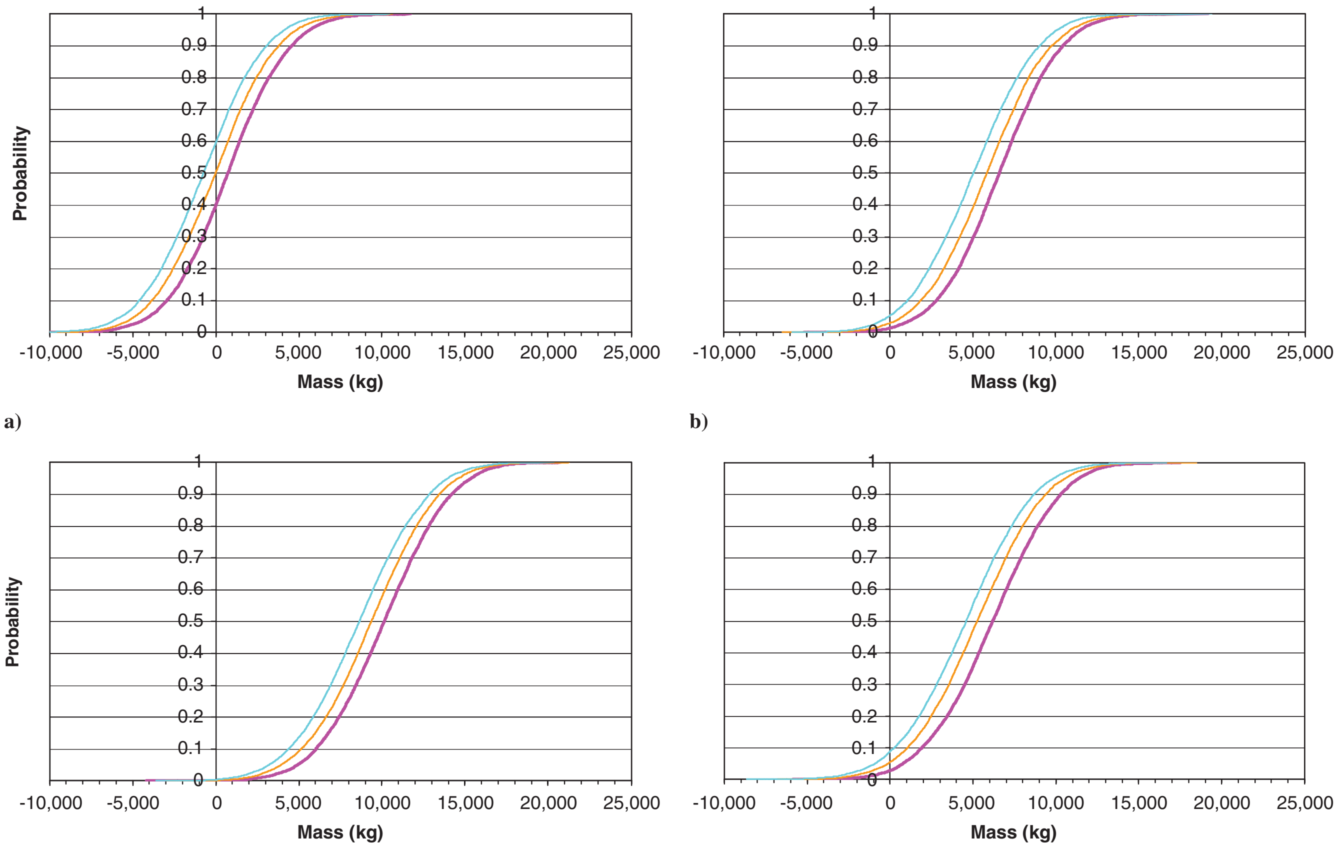

Fig. 7 CDFs from the Monte Carlo simulation of Ares-V/EDS gross payload-delivery capability less TLI stack mass for a) Ares-V/EDS vehicle 51.0.39, b) Ares-V/EDS vehicle 51.0.48, c) Ares-V/EDS vehicle 51.0.47, and d) Ares-V/EDS vehicle 51.0.47 with 2000 kg of additional descent module cargo/PMR. In all of the figures, Orion TLI mass was held fixed at 20,185 kg and 500 kg of basic payload was carried on Altair. The three *S* curves in each figure represent LOI Δv of 891, 950, and 1000 m/s, respectively, reading from bottom to top.

mass result and the beta distribution draw are combined in the Monte Carlo simulation engine to build the desired PDF.

To demonstrate the approach, cases of interest to the Constellation program were created and their results are reported here. First, basic mass estimates for one particular Altair design were available at the time of this analysis. This design, designated as p0804D, was structurally optimized for a crewed lunar sortie DRM with the DM propellant tanks sized for 1000 m/s. For this design, two parameters (LOI Δv and the amount of unpressurized cargo that could be carried on the DM) were systematically varied to see the effect on the probability that the Ares-V/EDS gross delivery capability exceeds the TLI stack mass. The LOI Δv was stepped from 891 to 950 to 1000 m/s. The low end of this range (891 m/s) represents the LOI requirement for a mission to an outpost at the lunar south pole, whereas the higher values would enable, in conjunction with LOI loiter, lunar sortie missions to a much greater percentage of the lunar surface. Access to most of the lunar surface (in particular, to a set of identified sites), is a Constellation program requirement. Further, each mission, independently of its destination on the lunar surface, is required to carry a minimum of 500 kg in unpressurized science cargo (including any accommodation mass). The amount of DM unpressurized cargo was varied from no additional cargo above the 500 kg minimum requirement to as much as 3000 kg above it. This additional cargo is fungible with dry mass PMR, because the propellant for it is included in the MassTracker calculation. Neither the minimum science cargo nor the additional cargo/PMR was subject to the mass growth of Eq. (5). At the time of the analysis, the Orion project was beyond SRR, though not yet at the PDR level of maturity. Instead of using the SRR mass growth model, the Orion TLI mass and spacecraft adapter mass were fixed at their respective then-current control masses, and so, in essence, all the results shown subsequently are based on stochastic variability in Altair's TLI mass and in Ares-V/EDS performance. In future analyses, a PDR mass growth model will be applied to Orion.

Figure 7 shows a group of Monte Carlo simulations results for $P^t_{\mathrm{EDS}} - M^t_{\mathrm{TLI}}$. Each simulation case was terminated at 10,000 trials, which was sufficient to ensure a statistically significant sample [76]. In Fig. 7a, the lowest performance Ares-V/EDS 51.0.39 is simulated with an Altair configuration carrying only the minimum science cargo of 500 kg. The critical probability ranges from approximately 0.4 to 0.6, depending on the LOI Δv for the DRM. Such a range indicates that dry mass growth poses a significant problem for this combination of launch vehicle and lunar lander. A vast improvement

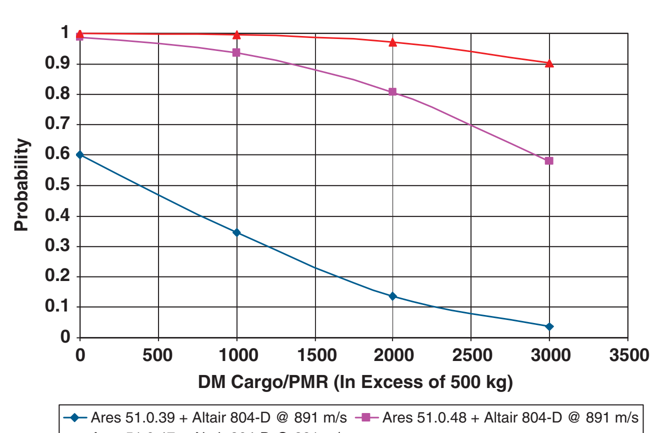

Fig. 8 Critical probabilities for various Ares-V/EDS designs and Altair loadings.

in the critical probability is seen in Fig. 7b, in which the Ares-V/EDS 51.0.48 launch vehicle is substituted. The critical probability ranges from approximately 0.95 to almost 0.99. In Figs. 7c and 7d, the highest-performance Ares-V/EDS 51.0.47 is simulated. With no additional DM cargo/PMR in Fig. 7c, the critical probability ranges from 0.996 to 0.999, depending on LOI Δv, and even with 2000 kg additional DM cargo/PMR, the critical probability ranges from 0.91 to 0.97.

Figure 8 is a plot of the critical probabilities for the lunar outpost DRM for the three Ares-V/EDS conceptual designs against varying quantities of additional DM cargo/PMR. This plot, which contains the same information available in Fig. 7, nevertheless shows how the 51.0.39 is not a viable option, even for the most basic lunar DRM with the minimum science cargo (the vertical axis).

IV. Conclusions

For the Constellation program, these critical probabilities are the end products of the analysis. The analysis results provide the program manager with some insights into the Ares-V/EDS and Altair conceptual designs that warrant further development and the amount of PgMR in Fig. 2 that provides sufficient robustness and flexibility in achieving program objectives. PgMR provides the program manager with control over a critical resource, but it cannot be arbitrarily used with respect to any constituent project or to cover mass issues at specific mission phases. For example, PgMR cannot necessarily be used to raise the control mass of Orion at lunar ascent target injection for the lunar DRM, because it could violate mass requirements at TLI and might also violate reentry limits, including thermal protection capabilities and center-of-mass limitations to achieve the necessary lift-over-drag ratio. Further, once the Orion design is set and the spacecraft is in production, use of PgMR to add a new capability may be prohibitively difficult or expensive to implement. Therefore, to understand the options for use of PgMR, specific analyses will be needed to assess program-level threats and opportunities and various uses of PgMR over the life cycle of the program. Based on these analyses, the program manager may choose to make specific allocations of PgMR by DRMs. Some examples of current and possible future PgMR allocations are additional propellant for the Orion SM for which the tanks are sized; additional flight crew and EVA equipment; additional payload carried to and/or returned from the moon; changes to accommodate design issues (e.g., thrust oscillation); and changes to increase operability, producibility, and maintainability.

Building in a larger PgMR at the outset of the Constellation program is not without cost. A larger PgMR may impose additional development and life-cycle cost and development risk on constituent projects by constraining solutions unnecessarily. A balance is needed between the effectiveness of a larger PgMR in meeting program objectives and its cost. Further, although deriving an optimal set of time-dependent program and project control masses from knowledge of the stochastic distributions would be extremely useful, that problem is left for future research.

The stochastic margins analysis reinforced other analyses that pointed toward the Ares-V/EDS 51.0.48 and 51.0.47 conceptual designs as viable options. With their greater performance than the 51.0.39, these conceptual designs open up a number of interesting possibilities for making use of the potential for increased DM cargo capability on both crewed missions and autonomously landed cargo missions. The stochastic margins analysis can be used to develop conditional probability distributions for this DM cargo capability, which will determine what kinds of exploration scenarios are logistically feasible.

The stochastic margins analysis described in this paper is being used in the Constellation program alongside the traditional mass margin control methods in [2]. By taking into account the uncertainty in spacecraft mass growth through milestone-dependent mass growth models and the uncertainty in launch vehicle gross payload-delivery capability, the analysis provides an integrated assessment of the mass margins distributed throughout the program. As the constituent projects progress through PDR and CDR, the spacecraft mass and performance probability distributions used in the stochastic assessment should evolve toward those with lower variance as information about designs improves and risks are mitigated. The stochastic assessment, by revealing the combined effects of decisions affecting mass, will continue to provide an important additional dimension to traditional methods in determining the overall health of the mass margins within the program. In particular, the approach described in this paper allows the set of current margins to be evaluated in terms of the probability of meeting the TLI performance and mass requirements for the Ares-V/EDS and other Constellation elements. The techniques discussed are also expected to find broad application in other complex system-of-systems space missions, including Mars sample return and human missions to Mars.

Appendix A: Gemini and Apollo Mass Histories from Quarterly Status Reports

Table A1 Gemini mass history from quarterly status reports (in kilograms): QSR 1 to QSR 8

Item	QSR 1[c] 31 May 1962	QSR 2 31 Aug. 1962	QSR 3 30 Nov. 1962	QSR 4 28 Feb. 1963	QSR 5 31 May 1963	QSR 6 31 Aug. 1963	QSR 7 30 Nov. 1963	QSR 8 29 Feb. 1964
Gross mass 14-day configuration[a]	3123.9	3148.8	3168.8	3270.0	3037.3	3078.1	3114.8	3272.7
Dry mass (estimated)[b]	2446.4	2471.4	2491.3	2592.5	2359.8	2400.6	2437.3	2595.2

[a]Spacecraft 7 designated as first of this configuration.
[b]Estimated based on gross mass less crew, estimated flight crew equipment, nonpropellant, and usable propellant mass.
[c]SRR at QSR 1.

Table A2 Gemini mass history from quarterly status reports (in kilograms): QSR 9 to QSR 16

Item	QSR 9 31 May 1964	QSR 10 31 Aug. 1964	QSR 11 30 Nov. 1964	QSR 12 28 Feb. 1965	QSR 13 31 May 1965	QSR 14 31 Aug. 1965	QSR 15 30 Nov. 1965	QSR 16 28 Feb. 1966
Gross mass 14-day configuration[a]	3197.4	3404.2	3418.3	3535.3	3541.2	3611.5	3648.2	3663.2
Dry mass (estimated)[b]	2519.9	2726.7	2740.8	2857.8	2863.7	2934.0	2970.8	2985.7

[a]Spacecraft 7 designated as first of this configuration.
[b]Estimated based on gross mass less crew, estimated flight crew equipment, nonpropellant, and usable propellant mass.

Table A3 Apollo mass history from quarterly status reports (in kilograms): QSR 1–QSR 6[a]

Item	QSR 1[c] 30 Sept. 1962	QSR 2 31 Dec. 1962	QSR 3 31 Mar. 1963	QSR 4 30 June 1963	QSR 5 30 Sept. 1963	QSR 6 31 Dec. 1963
Command module (with crew)	4,309.1	4,241.1	4,077.8	4,159.4	4,377.2	4,431.6
Estimated CM (without crew)	4,064.5	3,996.4	3,833.2	3,914.8	4,132.5	4,187.0
Service module	23,496.1	20,373.1	21,296.2	21,423.2	22,448.8	23,108.3
Inert (include residual propellant)	5,216.3	4,628.9	4,436.1	4,200.3	4,390.8	4,381.7
Usable SPS[b] propellant ($\Delta V = 3,870$ fps)	18,279.8	15,744 2	11,666.4	11,861.5	12,707.4	13,267.6
Usable SPS[b]propellant ($\Delta V = 3,915$ fps)	18,279.8	15,744 2	5,193.6	5,198.2	5,350.6	5,459.0
Total CSM	27,805.2	24,614.2	25,374.0	25,582.6	26,825.9	27,539.9
Dry CSM (estimated)	8,834.9	8,179.5	7,823.4	7,669.2	8,077.4	8,122.8
Lunar excursion module (without crew)	11,566.6	9,752.2	11,113.0	11,521.3	12,916.5	13,813.7
Descent stage inert	——	——	——	1,432.0	1,488.2	1,580.8
Usable propellant ($\Delta V = 7,827$ fps)	——	——	——	6,446.9	7,018.9	7,668.6
Ascent stage inert	——	——	——	1,652.0	2,445.3	2,268.0
Usable propellant ($\Delta V = 7,079$ fps)	——	——	——	1,990.4	1,963.6	2,311.1
Adapter to S-IVB	1,542.2	1,478.7	1,410.7	1,410.7	1,410.7	1,542.2
Total spacecraft injected weight	40,823.4	35,845.2	38,124.5	38,741.4	41,284.7	43,036.9
Launch escape system	2,993.7	——	2,903.0	2,898.5	3,016.4	3,272.7
Total launch weight	43,817.1	——	41,027.5	41,639.8	44,450.7	46,309.6

[a]Not all QSRs reported mass data. Before QSR 12, mass was reported in a standard table, which then appears only sporadically through QSR 25.
[b]SPS is the service propulsion system, $I_{sp} = 313$ s. Upper row is for lunar orbit insertion and lower row is for trans-Earth injection burn.
[c]Contains only "design allowable" values, not estimates.

Table A4 Apollo mass history from quarterly status reports (in kilograms): QSR 7–QSR 12[a]

Item	QSR 7 31 Mar. 1964	QSR 8 30 June 1964	QSR 9 30 Sept. 1964	QSR 10 31 Dec. 1964	QSR 11 31 Mar. 1965	QSR 12 30 June 1965
Command module (with crew)	4,554.1	4,549.5	4,576.8	4,567.7	4,694.7	——
Estimated CM (without crew)	4,309.4	4,304.9	4,332.1	4,323.6	4,450.0	——
Service module	20,842.6	21,207.7	21,452.2	21,391.4	21,754.3	——
Inert (include residual propellant)	4,513.2	4,590.4	4,558.6	4,581.3	4,526.9	——
Usable SPS[b] propellant ($\Delta V = 3,883$ fps)	12,022.5	12,276.5	12.554.1	12,510.1	12,832.1	——
Usable SPS[b]propellant ($\Delta V = 4,801$ fps)	4,306.9	4,340.9	4,339.5	4,345.4	4,395.3	——
Total CSM	25,396.7	25,757.3	26,029.6	25,959.1	26,449.0	——
Dry CSM (estimated)	8,376.8	8,449.3	8,444.8	8,458.4	8,531.0	——
Lunar excursion module (without crew)	12,314.6	12,314.6	13.349.7	13,236.3	13,768.4	——
Descent stage inert	1,655.6	1,723.7	1,808.5	1,798.9	1,933.7	——
Usable propellant ($\Delta V = 7,827$ fps)	6,650.6	6,883.3	7,219.8	7,163.1	7,436.6	——
Ascent stage inert	1,960.9	2,014.0	2,077.9	2,045.3	2,077.0	——
Usable propellant ($\Delta V = 7,079$ fps)	2,047.5	1,973.1	2,243.5	2,229.0	2,271.1	——
Adapter to S-IVB	1,542.2	1,576.2	1,678.3	1,678.3	1,553.6	——
Total spacecraft injected weight	39,253.5	40,081.7	41,057.0	40,919.1	41,770.9	——
Launch escape system	3,299.9	3,406.5	3,603.8	3,619.7	3,690.0	——
Total launch weight	42,553.4	43,486.9	44,660.8	44,538.7	45,460.9	——

[a]Not all QSRs reported mass data. Before QSR 12, mass was reported in a standard table, which then appears only sporadically through QSR 25.
[b]SPS is the service propulsion system, $I_{sp} = 313$ s. Upper row is for lunar orbit insertion and lower row is for trans-Earth injection burn.

Table A5 Apollo mass history from quarterly status reports (in kilograms): QSR 13–QSR 18[a]

Item	QSR 13 30 Sept. 1965	QSR 14 31 Dec. 1965	QSR 15[c] 31 Mar. 1966	QSR 16[d] 30 June 1966	QSR 17 30 Sept. 1966	QSR 18 31 Dec. 1966
Command module (with crew)	——	——	5,042.1	5,159.2	——	——
Estimated CM (without crew)	——	——	4,797.5	4,914.5	——	——
Service module	——	——	——	——	——	——
Inert (include residual propellant)	——	——	4,625.7	4,657.5	——	——
Usable SPS[b] propellant ($\Delta V = 3,870$ fps)	——	——	——	——	——	——
Usable SPS[b] propellant ($\Delta V = 3,915$ fps)	——	——	——	——	——	——
Total CSM	——	——	——	——	——	——
Dry CSM (estimated)	——	——	——	——	——	——
Lunar excursion module (without crew)	14,314.5	14,363.5	13,991.1	13,967.5	13,868.1	13,868.1
Descent stage inert	——	——	2,152.8	——	——	——
Usable propellant ($\Delta V = 7,827$ fps)	——	——	7,551.0	——	——	——
Ascent stage inert	——	——	1,999.0	——	——	——
Usable propellant ($\Delta V = 7,079$ fps)	——	——	2,288.4	——	——	——
Adapter to S-IVB	——	——	——	1,651.5	——	——
Total spacecraft injected weight	——	——	——	——	——	——
Launch escape system	——	——	——	3,798.8	——	——
Total launch weight	——	——	——	——	——	——

[a]Not all QSRs reported mass data. Before QSR 12, mass was reported in a standard table, which then appears only sporadically through QSR 25.
[b]SPS is the service propulsion system, $I_{sp} = 313$ s. Upper row is for lunar orbit insertion and lower row is for trans-Earth injection burn.
[c]Identified as CSM block II and as LEM-4.
[d]Identified as CSM-103 and subsequent.

Table A6 Apollo mass history from quarterly status reports (in kilograms): QSR 19–QSR 25[a]

Item	QSR 19 31 Mar. 1967	QSR 21 30 Sept. 1967	QSR 22 31 Dec. 1967	QSR 23[c] 31 Mar. 1968	QSR 24 30 June 1968	QSR 25 30 Sept. 1968
Command module (with crew)	——	——	5,838.6	5,681.3	——	——
Estimated CM (without crew)	——	——	5,594.0	5,436.6	——	——
Service module	——	——	22,925.0	23,329.2	——	——
Inert (include residual propellant)	——	——	4,898.8	5,213.6	——	——
Usable SPS[b] propellant ($\Delta V = 3,870$ fps)	——	——	18,026.2	18,115.6	——	——
Usable SPS[b] propellant ($\Delta V = 3,915$ fps)	——	——	——	——	——	——
Total CSM	——	——	28,763.7	29,010.4	——	——
Dry CSM (estimated)	——	——	10,046.9	10,204.3	——	——
Lunar excursion module (without crew)	——	——	14,797.6	14,823.9	——	——
Descent stage inert	——	——	2,225.8	2,160.0	——	——
Usable propellant ($\Delta V = 7,827$ fps)	——	——	——	7,942.4	——	——
Ascent stage inert	——	——	2,120.5	2,202.6	——	——
Usable propellant ($\Delta V = 7,079$ fps)	——	——	——	2,518.8	——	——
Adapter to S-IVB	——	——	1,769.0	1,732.3	——	——
Total spacecraft injected weight	——	——	45,330.3	45,566.6	——	——
Launch escape system	——	——	4,027.5	4,127.7	——	——
Total launch weight	——	——	49,357.7	49,694.3	——	——

[a]Not all QSRs reported mass data. Before QSR 12, mass was reported in a standard table, which then appears only sporadically through QSR 25.
[b]SPS is the service propulsion system, $I_{sp} = 313$ s. Upper row is for lunar orbit insertion and lower row is for trans-Earth injection burn.
[c]Detailed as CSM-107/LM-6 (lunar mission).

Appendix B: Dry Mass Growth from SRR

Table B1 Dry mass growth from SRR

Spacecraft	Basic dry mass at SRR, kg	Actual dry mass at launch, kg	Growth rate, %	Launch mass predicted by Eq. (4) with $\beta = 1.29719$	% error
Mars 2001 Lander/Phoenix	509	538	5.76	660.3	22.66
Mars Global Surveyor	529	593	12.24	685.8	15.58
Voyager	551	604	9.62	714.4	18.33
Dawn	543	701	28.96	704.6	0.59
Mars Reconnaissance Orbiter	600	822	37.02	778.2	−5.33
Magellan	778	899	15.68	1,008.6	12.14
Mercury	902	1,142	26.58	1,170.5	2.48
Cassini	1,158	1,753	51.34	1,502.7	−14.29
Topex/Poseidon	1,510	1,885	24.87	1,958.2	3.88
Viking Orbiter/Lander	1,437	2,232	55.38	1,863.4	−16.52
Gemini (14-day configuration)	2,446	2,864	17.06	3,173.4	10.82
Apollo: LEM	2,687	3,869	43.99	3,485.4	−9.91
Apollo: CSM	8,180	10,046	22.82	10,610.4	5.62
Hubble Space Telescope	8,582	10,857	26.51	11,132.5	2.54
SkyLab: Apollo Telescope Mount	8,417	11,155	32.53	10,918.4	−2.12
SkyLab: Orbital Workshop	22,450	35,380	57.59	29,122.9	−17.69
Skylab	54,500	76,295	39.99	70,697.9	−7.34
Space Shuttle Orbiter	60,618	76,985	27.00	78,633.1	2.14

Acknowledgments

The research described in this paper was carried out at the Jet Propulsion Laboratory (JPL), California Institute of Technology, under a contract with NASA. The authors wish to thank Brian J. Derkowski, Brett G. Drake, James R. Geffre, Kent B. Joosten, and Roland M. Martinez at the NASA Johnson Space Center (JSC); David M. Anderson, Geoff Beech, Stephen D. Creech, James B. Holt, and Grady E. Threet at the NASA Marshall Space Flight Center; Daniel D. Mazanak at the NASA Langley Research Center; Erick Sturm at the Jet Propulsion Laboratory; and Bradley St. Germain at SpaceWorks Engineering, Inc. Special thanks go to Jennifer Ross-Nazzal, JSC Historian, Christa George (JSC Scientific and Technical Information Center), and Rodney Krajca (National Archives and Records Administration), who located and provided electronic copies of Gemini and Apollo quarterly status reports. Many of these historic documents were difficult to locate and had to be converted to JPEG file formats page by page. Deborah R. Wills, Hedi C. Cox (Marshall Space Flight Center) and Ann S. Coppin (Jet Propulsion Laboratory) helped locate the original mass properties reports and other data for the Hubble Space Telescope. The unmanned spacecraft mass data were collected by Elizabeth Deems at the Jet Propulsion Laboratory and Skip Harvey at the Aerospace Corporation. The authors wish to thank them as well for their important contributions.

References

[1] Shishko, R., and Chamberlain, R. G., *NASA Systems Engineering Handbook*, NASA, Rept. SP-6105, 1995, pp. 61—63.
[2] *AIAA Standard—Mass Properties Control for Space Systems (S-120-2006)*, AIAA, Reston, VA, 2006.
[3] Hawkins, K., "Space Vehicle and Associated Subsystem Weight Growth," 47th Annual Conference of the Society of Allied Weight Engineers, Detroit, MI, International Society of Allied Weight Engineers Paper 1816, May 1988.
[4] Wilhite, A. W., Reeves, D., Stanley, D. O., and Wagner, J., "Evaluating the Impacts of Mass Uncertainty on Future Exploration Architectures," AIAA Paper 2006-7250, Sept 2006.
[5] Kim, D. J., Wilson, J., Chiang, J., and Hom, S., "SS/L Historical Trends on Satellite Mass Growth," 25th AIAA International Communications Satellite Systems Conference, Seoul, ROK, AIAA Paper 2007-3220, Apr. 2007.

[6] White, T. A., “RS-68 Weight History and Predicted Flight Weight,” 58th Annual Conference of the Society of Allied Weight Engineers, San Jose, CA, International Society of Allied Weight Engineers Paper 2451, May 1999.
[7] “Sequence and Flow of Hardware Development and Key Inspection, Review and Certification Checkpoints,” *Apollo Program Directive No. 6*, Office of Manned Space Flight, MA 1400.006, Washington, D.C., 12 Aug. 1965.
[8] “Project Apollo Quarterly Status Report No. 4,” NASA Manned Spacecraft Center NASA-TM-X-66740, Houston, TX, 30 June 1963, p. 28.
[9] Faget, M. A., Garland, B., and Buglia, J. J., “Preliminary Studies of Manned Satellites, Wingless Configuration, Non-Lifting,” NACA, 18 Mar. 1958; Reissued as NASA TN D-1254, Mar. 1962.
[10] Swenson, L. S., Jr., Grimwood, J. M., and Alexander, C. C., *This New Ocean: A History of Project Mercury*, NASA SP-4201, 1989, Chap. 7, footnote 64.
[11] Korando, R. D., “Mercury Capsule No. 2 Configuration Specification (Mercury-Redstone No. 1),” McDonnell Aircraft Corp. Rept. 6603-2, St. Louis, MO, 2 June 1960; revised 6 Feb. 1961, p. 9; available online at http://ntrs.nasa.gov/archive/nasa/casi.ntrs.nasa.gov/19740075935_1974075935.pdf [retrieved 20 July 2009].
[12] “Project Mercury Status Report No. 9,” NASA Manned Spacecraft Center, NASA-TM-X-70167, Houston TX, 31 Jan. 1961.
[13] “Project Mercury Status Report No. 12,” NASA Manned Spacecraft Center, NASA-TM-X-5048, Houston TX, 31 Oct. 1961.
[14] “Project Mercury Quarterly Status Report No. 14,” NASA Manned Spacecraft Center, NASA-TM-X-69214, Houston TX, 30 Apr. 1962.
[15] “Project Mercury Quarterly Status Report No. 19,” NASA Manned Spacecraft Center, NASA-TM-X-69235, Houston TX, 31 July 1963.
[16] ”Postlaunch Memorandum Report for Mercury-Atlas No. 5 (MA-5),” NASA Manned Spacecraft Center, NASA-TM-X-69533, Cape Canaveral, FL, 6 Dec. 1961, p. 3-2.
[17] “Project Gemini Quarterly Status Report No. 1,” NASA Manned Spacecraft Center, Houston, TX, 31 May 1962
[18] “Project Gemini Quarterly Status Report No. 2,” NASA Manned Spacecraft Center, Houston, TX, 31 Aug. 1962
[19] “Project Gemini Quarterly Status Report No. 3,” NASA Manned Spacecraft Center, Houston, TX, 30 Nov. 1962
[20] “Project Gemini Quarterly Status Report No. 4,” NASA Manned Spacecraft Center, Houston, TX, 28 Feb. 1963
[21] “Project Gemini Quarterly Status Report No. 5,” NASA Manned Spacecraft Center, Houston, TX, 31 May 1963
[22] “Project Gemini Quarterly Status Report No. 6,” NASA Manned Spacecraft Center, Houston, TX, 31 Aug. 1963
[23] “Project Gemini Quarterly Status Report No. 7,” NASA Manned Spacecraft Center, Houston, TX, 30 Nov. 1963
[24] “Project Gemini Quarterly Status Report No. 8,” NASA Manned Spacecraft Center, Houston, TX, 29 Feb. 1964
[25] “Project Gemini Quarterly Status Report No. 9,” NASA Manned Spacecraft Center, Houston, TX, 31 May 1964
[26] “Project Gemini Quarterly Status Report No. 10,” NASA Manned Spacecraft Center, Houston, TX, 31 Aug. 1964
[27] “Project Gemini Quarterly Status Report No. 11,” NASA Manned Spacecraft Center, Houston, TX, 30 Nov. 1964
[28] “Project Gemini Quarterly Status Report No. 12,” NASA Manned Spacecraft Center, Houston, TX, 28 Feb. 1965
[29] “Project Gemini Quarterly Status Report No. 13,” NASA Manned Spacecraft Center, Houston, TX, 31 May 1965
[30] “Project Gemini Quarterly Status Report No. 14,” NASA Manned Spacecraft Center, Houston, TX, 31 Aug. 1965
[31] “Project Gemini Quarterly Status Report No. 15,” NASA Manned Spacecraft Center, Houston, TX, 30 Nov. 1965
[32] “Project Gemini Quarterly Status Report No. 16,” NASA Manned Spacecraft Center, Houston, TX, 28 Feb. 1966
[33] “Gemini Spacecraft Program Quarterly Status Report No. 17,” NASA Manned Spacecraft Center, Houston, TX, 31 May 1966.
[34] “Gemini Program Quarterly Status Report No. 18,” NASA NASA Manned Spacecraft Center, Houston, TX, 31 Aug. 1966.
[35] “Project Apollo Quarterly Status Report No. 1,” NASA Manned Spacecraft Center, Houston, TX, 30 Sept. 1962
[36] “Project Apollo Quarterly Status Report No. 2,” NASA Manned Spacecraft Center, Houston, TX, 31 Dec. 1962
[37] “Project Apollo Quarterly Status Report No. 3,” NASA Manned Spacecraft Center, Houston, TX, 31 Mar. 1963
[38] “Project Apollo Quarterly Status Report No. 4,” NASA Manned Spacecraft Center, Houston, TX, 30 June 1963
[39] “Project Apollo Quarterly Status Report No. 5,” NASA Manned Spacecraft Center, Houston, TX, 30 Sept. 1963
[40] “Project Apollo Quarterly Status Report No. 6,” NASA Manned Spacecraft Center, Houston, TX, 31 Dec. 1963
[41] “Project Apollo Quarterly Status Report No. 7,” NASA Manned Spacecraft Center, Houston, TX, 31 Mar. 1964
[42] “Project Apollo Quarterly Status Report No. 8,” NASA Manned Spacecraft Center, Houston, TX, 30 June 1964
[43] “Project Apollo Quarterly Status Report No. 9,” NASA Manned Spacecraft Center, Houston, TX, 30 Sept. 1964
[44] “Apollo Spacecraft Program Quarterly Status Report No. 10,” NASA Manned Spacecraft Center, Houston, TX, 31 Dec. 1964
[45] “Apollo Spacecraft Program Quarterly Status Report No. 11,” NASA Manned Spacecraft Center, Houston, TX, 31 Mar. 1965
[46] “Apollo Spacecraft Program Quarterly Status Report No. 12,” NASA Manned Spacecraft Center, Houston, TX, 30 June 1965
[47] “Apollo Spacecraft Program Quarterly Status Report No. 13,” NASA Manned Spacecraft Center, Houston, TX, 30 Sept. 1965
[48] “Apollo Spacecraft Program Quarterly Status Report No. 14,” NASA Manned Spacecraft Center, Houston, TX, 31 Dec. 1965
[49] “Apollo Spacecraft Program Quarterly Status Report No. 15,” NASA Manned Spacecraft Center, Houston, TX, 31 Mar. 1966
[50] “Apollo Spacecraft Program Quarterly Status Report No. 16,” NASA Manned Spacecraft Center, Houston, TX, 30 June 1966
[51] “Apollo Spacecraft Program Quarterly Status Report No. 17,” NASA Manned Spacecraft Center, Houston, TX, 30 Sept. 1966
[52] “Apollo Spacecraft Program Quarterly Status Report No. 18,” NASA Manned Spacecraft Center, Houston, TX, 31 Dec. 1966
[53] “Apollo Spacecraft Program Quarterly Status Report No. 19,” NASA Manned Spacecraft Center, Houston, TX, 31 Mar. 1967
[54] “Apollo Spacecraft Program Quarterly Status Report No. 21,” NASA Manned Spacecraft Center, Houston, TX, 30 Sept. 1967
[55] “Apollo Spacecraft Program Quarterly Status Report No. 22,” NASA Manned Spacecraft Center, Houston, TX, 31 Dec. 1967
[56] “Apollo Spacecraft Program Quarterly Status Report No. 23,” NASA Manned Spacecraft Center, Houston, TX, 31 Mar. 1968
[57] “Apollo Spacecraft Program Quarterly Status Report No. 24,” NASA Manned Spacecraft Center, Houston, TX, 30 June 1968
[58] “Apollo Spacecraft Program Quarterly Status Report No. 25,” NASA Manned Spacecraft Center, Houston, TX, 30 Sept. 1968
[59] “Weight Control and Weight Histories Report,” NASA Marshall Space Flight Center, Rept. RPT-1553A, Huntsville, AL, July 1991.
[60] Heacock, R., “The Voyager Spacecraft,” *Proceedings of the Institution of Mechanical Engineers*, Vol. 194, No. 28, June 1980, pp. 211–224. doi:10.1243/PIME_PROC_1980_194_026_02
[61] “Topex NASA Cost Update Review,” Vol. 1, Jet Propulsion Lab., Pasadena, CA, June 1985.
[62] “Topex/Poseidon Project, Satellite Resource and Margin Management Report,” Rept. 17, Fairchild Industries, Germantown, MD, 1 Apr. 1991.
[63] “Design Mass Properties: Guidelines and Formats For Aerospace Vehicles,” NASA Johnson Space Center, Rept. 23303, Houston, TX, Mar. 1989.
[64] “Design Mass Properties 2: Mass Estimating and Forecasting for Aerospace Vehicles Based on Historical Data,” NASA Johnson Space Center, Rept. 26098, Houston, TX, Nov. 1994.
[65] “Hubble Space Telescope Mass Properties Report,” ST/SE-04, Lockheed Missiles and Space Co., Inc., Rept. F130885, Sunnyvale, CA, 26 Sept. 1986.
[66] “Hubble Space Telescope Mass Properties Report,” ST/SE-04, Lockheed Missiles and Space Co., Inc., Rept. F297147A, Sunnyvale, CA, 23 Mar. 1990.
[67] “PRR Studies Results,” *Ferdinand Hamburger Archives*, The Johns Hopkins Univ., Collection 7, Hubble Space Telescope, Series 4, Box 3, Baltimore, MD, 27 June 1978.
[68] Anderson, T. W., and Darling, D. A., “Asymptotic Theory of Certain ‘Goodness-of-Fit’ Criteria Based on Stochastic Processes,” *Annals of Mathematical Statistics*, Vol. 23, 1952, pp. 193–212. doi:10.1214/aoms/1177729437
[69] *NIST/SEMATECH e-Handbook of Statistical Methods*, http://www.itl.nist.gov/div898/handbook [online book] [retrieved 9 July 2009].
[70] Oh, D. Y., Easter, R., Heeg, C., Sturm, E., Wilson, T., Woolley, R., and Rapp, D., “An Analytical Tool for Tracking and Visualizing the Transfer of Mass at Each Stage of Complex Missions,” AIAA Paper 2006-7254, Sept. 2006.
[71] “NASA Exploration Systems Architecture Study Final Report,” NASA TM-2005-214062, Nov. 2005, pp. 115–116, 164–165.
[72] Brauer, G. L., Cornick, D. E., and Stevenson, R., “Capabilities and Applications of the Program to Optimize Simulated Trajectories (POST),” NASA CR-2770, Feb. 1977.
[73] Wallace, J., St. Germain, B., and Charania, A., “Probabilistic Examinations of Lunar Landers,” AIAA Paper 2005-6734, Aug. 2005.

[74] Batson, R. G., "Program Risk Analysis Handbook," NASA TM-100311, Aug. 1987.
[75] Keefer, D. L., and Verdini, W. A., "Major Improvements in PERT via Better Three-Point Approximations," Arizona State Univ., Dept. of Decision and Information Systems, TR DIS 90/91-5, Tempe, AZ, Jan. 1991.
[76] Morgan, M. G., and Henrion, M., *Uncertainty: A Guide to Dealing with Uncertainty in Quantitative Risk and Policy Analysis*, Cambridge Univ. Press, Cambridge, England, U.K., 1990, pp. 198–203.

O. de Weck
Associate Editor